

Plant-derived Synthesis of Iron Oxide Nanoparticles for Magnetic Hyperthermia and Magnetic Resonance Imaging Applications

Mohamed Abdelmonem^{1,2}, Romesa Soomro¹, Norazalina Saad³, Mohamed Ahmed Ibrahim^{2,4}, Kim Wei Chan⁴, Emmellie Laura Albert⁵, Emma Ziezie Tarmizie⁶, Che Azurhanim Che Abdullah¹✉

¹ Department of Physics, Faculty of Science, Universiti Putra Malaysia, 43400 UPM Serdang, Malaysia

² Department of Pharmaceutics, Faculty of Pharmacy, October University for Modern Sciences and Arts, Giza, Egypt

³ Laboratory of Cancer Research UPM-MAKNA (CANRES), Institute of Bioscience, Universiti Putra Malaysia, 43400 UPM Serdang, Malaysia

⁴ Natural Medicines and Products Research Laboratory, Institute of Bioscience, Universiti Putra Malaysia, 43400 UPM Serdang, Malaysia

⁵ Nanomaterials Synthesis and Characterization Laboratory, Institute of Nanoscience and Nanotechnology, Universiti Putra Malaysia, 43400 UPM Serdang, Malaysia

⁶ Centre for Foundation Studies in Science, Universiti Putra Malaysia, 43400 UPM Serdang, Malaysia

✉ Corresponding author. E-mail: azurhanim@upm.edu.my

Received: Aug. 2, 2024; **Revised:** Aug. 22, 2024; **Accepted:** Sep. 14, 2024

Citation: M. Abdelmonem, R. Soomro, N. Saad, et al. Plant-derived synthesis of iron oxide nanoparticles for magnetic hyperthermia and magnetic resonance imaging applications. *Nano Biomedicine and Engineering*, 2025, 17(1): 74–90.

<http://doi.org/10.26599/NBE.2024.9290097>

Abstract

The biomedical applications of iron oxide nanoparticles (IONPs) synthesized using environmentally friendly processes are extremely promising. Using eco-friendly and nontoxic methods is a safer alternative to conventional chemical synthesis, which generates toxic byproducts. It allows for greater control over particle size and morphology. The resulting unique magnetic and optical properties of IONPs enable their use in biomedical applications such as magnetic hyperthermia (MH) and magnetic resonance imaging (MRI). This review aimed to summarize recent advances in the synthesis, characterization, and biosafety of IONPs for use in MH and MRI. It also aimed to highlight the significance of eco-friendly synthesis techniques for producing IONPs with the desired magnetic and physicochemical properties. Overall, this review elucidated the most efficient methods for utilizing iron oxide while considering biocompatibility.

Keywords: green chemistry; iron oxide nanoparticles (IONPs); magnetic resonance imaging (MRI); magnetic hyperthermia

Introduction

Nanotechnology is a rapidly expanding scientific field that has achieved significant success in the contemporary era. Nanoparticles (NPs) are one-of-a-kind materials distinguished by their small size

(typically 1–100 nm), structure, physical and chemical characteristics, electrical and magnetic behaviors, thermal responses, mechanical robustness, catalytic efficiencies, optical qualities, and shape [1–8]. Moreover, their properties and reactivity are typically defined by their small size and large surface

area [9–11]. Among all types of NPs, metal oxides are the most prominent and have been the subject of extensive research across diverse scientific fields. Due to their multifaceted properties, they have been explored for various applications and have significantly influenced various domains, such as electronics, catalysis, environmental science, medicine, and materials chemistry. Metal oxide NPs offer unique properties and functionalities that make them valuable in numerous applications, contributing to advancements in various scientific disciplines. Their versatile nature and potential for tailored modifications make them an essential focus of research and development efforts [12]. Recently, significant emphasis has been placed on their use in biomedical engineering, particularly for drug delivery, cancer therapy, and biomedical imaging. These efforts aim to produce metal oxide NPs with enhanced properties, making them more suitable for biomedical applications [12, 13].

Iron oxide NPs (IONPs) hold considerable importance among metal oxide NPs due to their exceptional magnetic characteristics, making them essential materials for various biomedical applications, including magnetic hyperthermia (MH) and magnetic resonance imaging (MRI). MH involves

using IONPs to generate localized heat when exposed to an alternating magnetic field. This heat can selectively destroy cancer cells without damaging surrounding healthy tissue, making MH a promising treatment option for various cancer types. Additionally, IONPs are widely used as contrast agents (CAs) in MRI, significantly improving tumor visualization and aiding in accurate diagnosis. Both MRI and MH will be discussed in detail in subsequent sections. These NPs are also being explored in targeted drug delivery systems, in which their magnetic properties can help guide therapeutic agents directly to cancer cells, reducing systemic toxicity and improving treatment outcomes. Figure 1 shows various IONP applications [14, 15].

IONPs comprise three significant phases: magnetite (Fe_3O_4), maghemite ($\gamma\text{-Fe}_2\text{O}_3$), and hematite ($\alpha\text{-Fe}_2\text{O}_3$). These oxides have a crystal structure characterized by closely packed planes of oxygen anions and interstitial spaces occupied by iron cations in either octahedral or tetrahedral coordinates [16]. Magnetite is a unique iron oxide with a face-centered cubic spinel structure. It comprises 32 closely packed oxygen ions. Unlike other iron oxides, magnetite contains a combination of divalent and trivalent iron ions. The Fe^{2+} ions occupy half of the

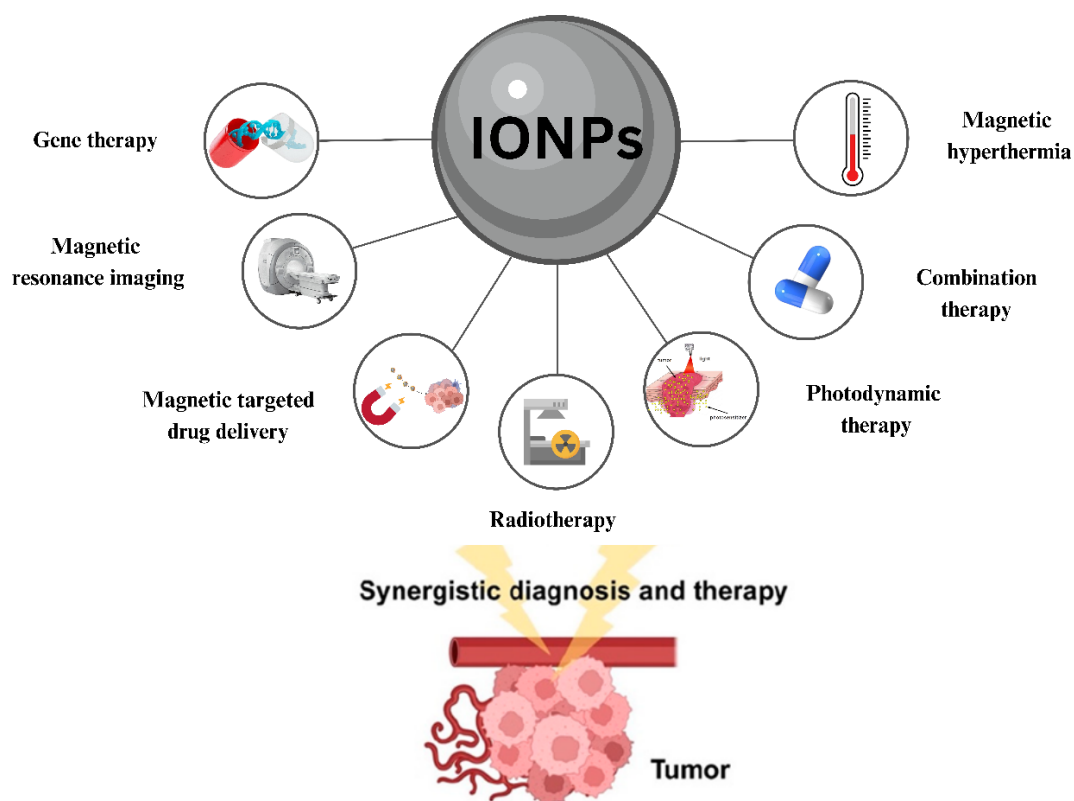


Fig. 1 Different biomedical applications of IONPs.

octahedral sites, whereas the Fe^{3+} ions are distributed evenly between the remaining octahedral and tetrahedral sites. Conversely, maghemite has a cubic structure. Each maghemite unit comprises 32 oxygen ions, $21\frac{1}{3}$ Fe^{3+} ions, and $2\frac{2}{3}$ vacancies. The cubic close packing of the oxygen anions creates the cubic structure, and the ferric ions are positioned at tetrahedral (eight ions per unit cell) and octahedral (comprising the remaining ions and vacancies) sites. Consequently, maghemite can be regarded as a fully oxidized magnetite. Hematite is considered the most stable of all iron oxides. It can significantly resist corrosion. Hematite can also serve as a starting material for synthesizing both magnetite and maghemite. The occurrence of IONPs in nanoform has imparted new magnetic, optical, and electrical properties to these materials, contributing to the phenomenon of quantum-size effects [14–16].

Furthermore, the superparamagnetic behavior of IONPs improves with decreasing size. However, their ferromagnetic behavior declines with decreasing size [17]. Therefore, IONPs with size of 10–20 nm exhibit the favorable superparamagnetic characteristics of magnetite and maghemite. Therefore, these materials can be used in various biomedical applications, including biosensors, drug delivery systems, electrical devices, CAs, and MH, for cancer treatment. These applications are primarily due to their high biocompatibility, outstanding stability, biodegradability, non-toxicity, and cost-effective preparation methods [18].

Although numerous chemical and physical methods exist for producing IONPs, these methods are limited by the requirement for hazardous chemicals [19]. Green techniques are considered more suitable because they significantly reduce the use and production of toxic substances during IONP synthesis [20]. Unmodified IONPs tend to exhibit low biocompatibility in highly acidic environments or after excessive exposure, resulting in reactivity, leaching, and degradation. Their superparamagnetic behavior and strong magnetic dipole-dipole attraction cause them to agglomerate, reducing their reusability and lifespan [19, 20]. Therefore, surface modification is necessary to enhance their stability and biocompatibility. Moreover, the colloidal suspension of unmodified IONPs, especially magnetite, which is susceptible to oxidation in air, causing significant loss of magnetism and dispersibility, can be stabilized by coating the surface with polymers containing

functional groups such as (R–COOH) or (R–NH₂) and having a high molecular weight [21, 22].

Despite the extensive literature on the biomedical applications of IONPs synthesized from various plants, a significant research gap exists in the use of green synthesized IONPs for MH and MRI. This research gap limits their potential as alternatives in biomedical practice. Furthermore, although the biocompatibility of plant-synthesized IONPs has been conducted, confirming their biosafety is crucial for clinical translation. Therefore, it is essential to investigate recent methods for MH and MRI using green synthesized IONPs while addressing their biocompatibility and scalability to ensure their safe, efficient, and industrially viable use in biomedical applications.

IONPs Synthesis

There are two main methods for synthesizing NPs: top-down and bottom-up methods. The top-down method relies on the fragmentation of larger structures into minute pieces, whereas the bottom-up method begins at the atomic level and employs chemical, physical, and biological techniques to fabricate NPs of the desired size. Figure 2 shows examples of both bottom-up and top-down methods [23, 24]. The biosynthesis pathway is a technique associated with the bottom-up method. The nanostructures produced via this method are considered safe, nontoxic, biocompatible, and environmentally friendly for use in biomedical applications [25, 26]

Top-down method

This method uses several lithographic techniques, including milling, crushing, and sputtering, to reduce the size of bulk material to tiny units. NPs produced using this method are typically irregular in shape and extremely small [25]. Consequently, the lack of suitable particle size and shape is the primary disadvantage of this method [26].

Bottom-up method

This method is the opposite of the top-down method. Nanostructures produced using this technique typically exhibit favorable shapes, sizes, and chemical compositions. They are fabricated from the bottom-up through the growth and self-assembly of atoms and molecules as building blocks [27]. Table 1

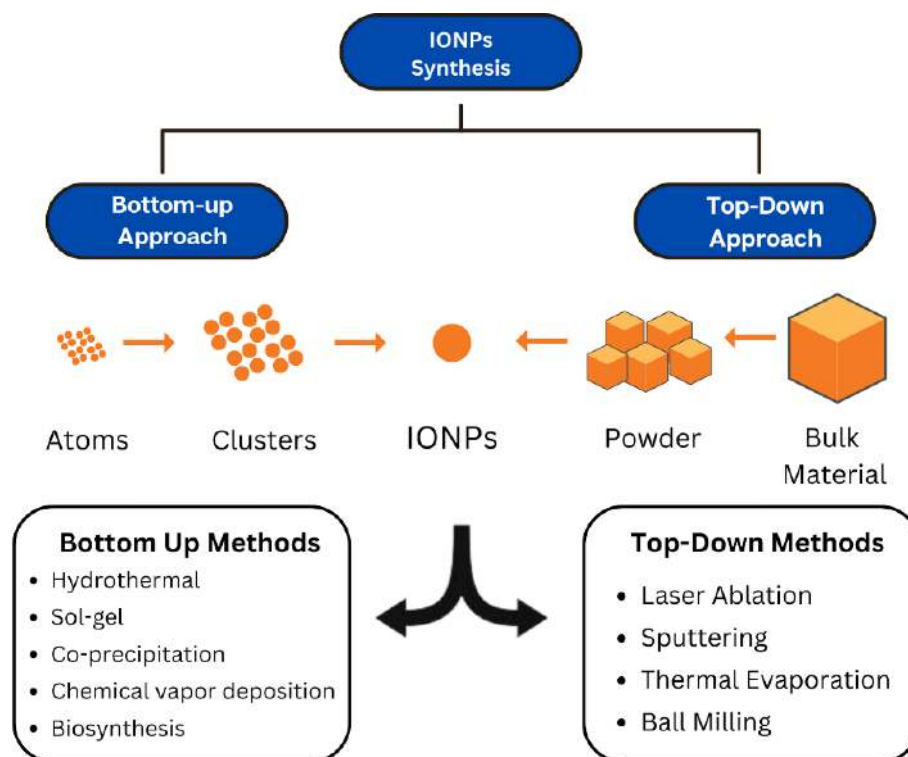


Fig. 2 Bottom-up and top-down methods of iron oxide nanoparticles (IONPs) synthesis.

presents the advantages and disadvantages of both top-down and bottom-up methods [25, 28–34].

IONPs Biosynthesis

The green synthesis method uses plant extracts, bacteria, viruses, yeasts, and fungi to produce nanomaterials from biological sources. These biological sources serve as eco-friendly precursors for

making stable, nontoxic nanoparticles (NPs), marking a significant advancement in the eco-friendly production of nanomaterials in nanotechnology. Due to the stabilizing and capping capabilities of biomolecules, particularly those derived from plant sources, these “green synthesized” NPs exhibit decreased toxicity and increased stability [35, 36]. Figure 3 shows the benefits of green IONP synthesis.

Table 1 The advantages and disadvantages of the Top-down and Bottom-up methods.

Approach	Method	Advantages	Disadvantages	Ref.
Top-down	Ball milling	<ul style="list-style-type: none"> • High capacity • Simplicity, reliability, and safety • Reduces the thickness of stacked materials 	<ul style="list-style-type: none"> • Inconvenient and heavy • Destruction and disordering of the chemical structure • High energy consumption due to grinding, heating, and friction 	[28]
	Thermal evaporation	<ul style="list-style-type: none"> • Suitable for materials with low melting point • Requires no solvent • Easy monitoring and control of the deposited material 	<ul style="list-style-type: none"> • Poor source material quality • Complex deposition of material combinations • Poor control of film property 	[29]
	Laser ablation	<ul style="list-style-type: none"> • Can produce ligand-free noble NPs in various solvents • Minimal energy loss 	<ul style="list-style-type: none"> • Need high energy for greater ablation efficacy • Even the most widely spread laser sources cannot produce NPs at an industrial scale • Ablation efficacy decreases with ablation time owing to the vast number of NPs scattered along the laser beam 	[25]
	Sputtering	<ul style="list-style-type: none"> • Works at low temperature • All elements, alloys, and compounds can be sputtered • Can coat large areas more uniformly 	<ul style="list-style-type: none"> • Low purity • Low sputtering rate compared with thermal evaporation • Most of the energy is converted to heat 	[30]

(To be continued on the next page)

Table 1 (Continued)

Approach	Method	Advantages	Disadvantages	Ref.
Bottom-up	Chemical vapor deposition	<ul style="list-style-type: none"> • Materials produced are dense and pure • High degree of control • Growth rate can be regulated easily 	<ul style="list-style-type: none"> • Some precursors are poisonous, flammable, and costly • Very poisonous gaseous byproducts are formed • High production costs 	[31]
	Hydrothermal method	<ul style="list-style-type: none"> • Accurate control of NP size • Fabrication of nanocrystals with high crystallinity • Low melting point and high vapor pressure 	<ul style="list-style-type: none"> • Expensive autoclave • Information on crystal growth cannot be observed directly 	[32]
	Co-precipitation	<ul style="list-style-type: none"> • Easy and quick to prepare • Energy-efficient and low-temperature usage • Easy modification of the particle surface 	<ul style="list-style-type: none"> • Difficult to control • Unsuitable if reactants have different precipitation rates • Impurities may be precipitated along with products 	[33]
	Sol-gel	<ul style="list-style-type: none"> • Cost-effective • Homogenous materials are produced • High purity • Low-temperature usage 	<ul style="list-style-type: none"> • Generates hazardous waste from chemical use • Relatively longer reaction time • The presence of organic chemicals influences health risk • Post-treatment is necessary for sample purification 	[34]

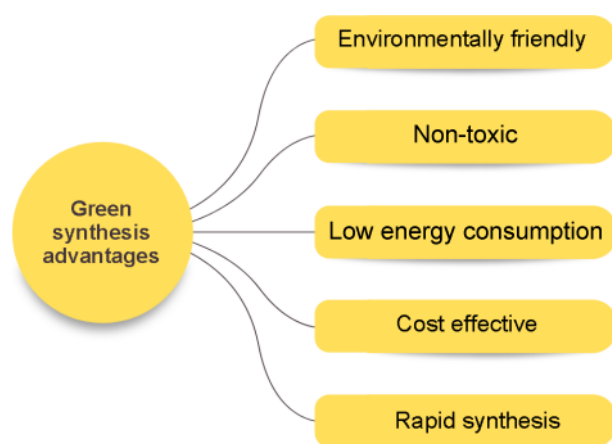


Fig. 3 Advantages of adopting green synthesis for the manufacturing of different nanoparticles.

Phytochemicals found in plant extracts play a crucial role in NP synthesis. Flavonoids, water-soluble plant secondary metabolites, exhibit oxygen-scavenging properties due to their electron-donating capacity. Phenolic compounds, including caffeic, protocatechuic, and gallic acids, form bonds with various metallic ions. Because of their reactive functional groups, terpenoids, proteins, organic acids, and alkaloids function as bio-reductants and stabilizers in nanomaterial formation [37].

Mechanism underlying IONPs Biosynthesis

Green nanoparticle synthesis comprises three stages:

reduction, growth, and termination. During reduction, the phytochemicals in the extract use electrostatic forces to reduce the metallic ions. During growth, metal atoms are separated from their metal precursors and assembled into NPs, while any remaining metallic ions are reduced. This forms NPs with stable morphologies; however, prolonged reduction may lead to irregular structures. During termination, biomolecules stabilize and cap the NPs [38]. Figure 4 shows the general scheme of the green IONP synthesis. The number of biomolecules significantly influences the final structure of synthesized NPs, as demonstrated by the use of green, oolong, and black tea extracts in IONP synthesis [39]. In a previous study, the green synthesis of iron nanomaterials was performed as follows: A ferric chloride solution was combined with guava extract to initiate a chelating reaction. The Fe^{3+} ions combined with the extract's phenolic group to form a complex, subsequently reduced to produce iron NPs. To prevent precursor solution oxidation, the synthesis was performed, and the synthesized product was stored in a nitrogen atmosphere [40]. Table 2 summarizes the previous research on IONP synthesis.

Advantages of green-synthesized IONPs

The quality of green-synthesized metal NPs surpasses that of those produced through chemical methods. For instance, magnetite NPs synthesized via green methods have particle sizes of 2–80 nm, significantly smaller than the 87–400-nm particles produced via

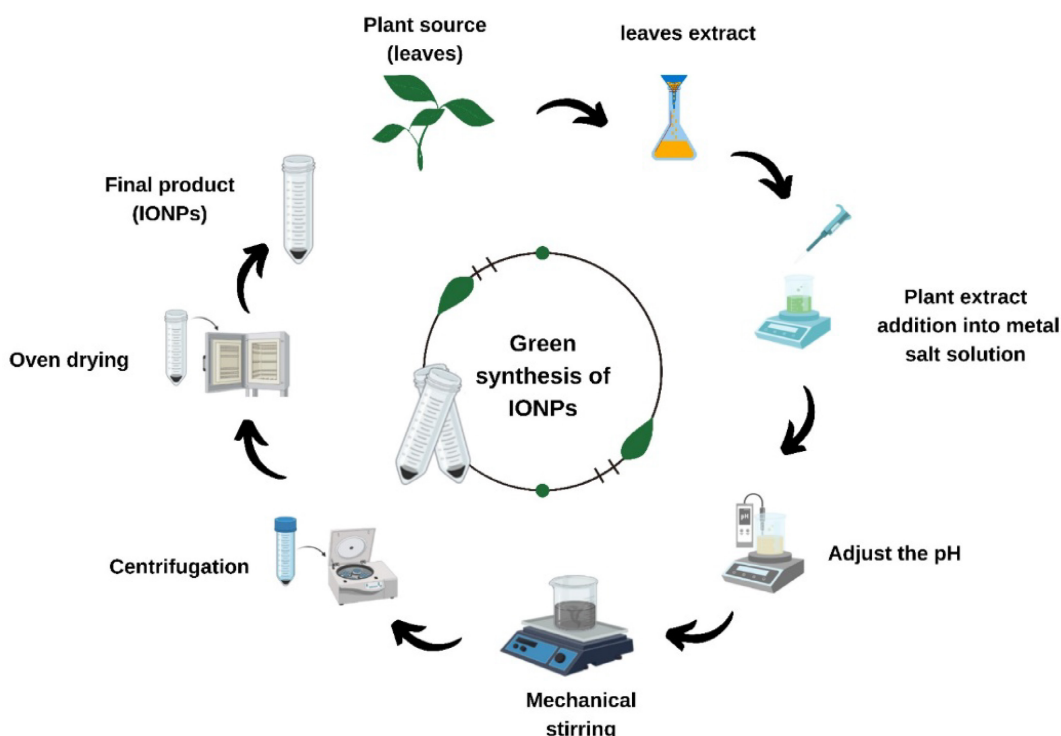


Fig. 4 General mechanism underlying the green synthesis of iron oxide nanoparticles (IONPs).

wet chemical methods [67]. The scalability of green synthesis is a key consideration for its application in industrial settings, and recent advancements have yielded promising results. Additionally, green synthesis offers benefits, including biocompatibility, potential in biological and medical applications, methodological simplicity, the use of natural resources, and non-toxicity, making synthesized NPs well-suited for pharmaceutical and biomedical purposes. Green synthesis is also cost-effective because it requires minimal or negligible energy inputs [68]. Due to their large surface area, NPs can have a high loading capacity, enabling even small dosages to be highly effective when active phytochemicals are attached. Their small size allows them to bypass cellular barriers and exploit the increased permeability and retention effect in diseased cells, an ability that bulk materials cannot achieve [69].

***In vitro* Toxicity Evaluation of Green-Synthesized IONPs**

IONPs are introduced into the human body for various medical applications, including MH and MRI contrast enhancement. Therefore, evaluating their biocompatibility is crucial. Numerous studies using

green chemistry approaches for synthesizing these NPs have confirmed their biocompatibility. Moreover, these polyphenol-coated IONPs are safe for MH treatments and as MRI CAs, exhibiting negligible adverse effects upon administration [67–71]. Table 3 enumerates previous studies on plant-mediated IONPs tested in various cell lines [72–78]. Therefore, *in vitro* cytotoxicity tests are used to assess the cytotoxicity and biocompatibility of various nanomaterials. These tests use cell cultures because they are safe, cost-effective, quick to respond, and, most importantly, easy to reproduce [67]. LDH, MTT, and MTS assays are frequently used methods for evaluating IONP toxicity on cell lines [73]. For instance, Dowlath et al. conducted a study using *Cardiospermum halicacabum* plant extract for the green synthesis (GS) of IONPs [69]. The toxicity of these NPs was assessed in comparison with chemically synthesized (CS) IONPs using human peripheral blood mononuclear cells (PBMCs). The GS-IONPs maintained $84.04\% \pm 0.94\%$ PBMC viability at a concentration of $100 \mu\text{g}\cdot\text{mL}^{-1}$, meeting the non-toxicity criteria set by ISO standards. Contrarily, the CS-IONPs significantly reduced PBMC viability, with only $53.68\% \pm 1.50\%$ viability at the same concentration [74]. Similarly, Sheel et al. explored the biocompatibility and toxicity of IONPs synthesized from *Phyllanthus niruri* leaf extract (P-

Table 2 Synthesis of iron oxide nanoparticles (IONPs) using different plant extracts.

Plant Name	Part of the plant used	Ion precursor	Size (nm)	Shape	Magnetization (emu·g ⁻¹)	Application	Ref.
<i>Bauhinia tomentosa</i>	Leaves	FeCl ₃	70	Spherical	55.83	Enzyme catalysis	[41]
<i>Canthium coromandelicum</i>	Leaves	FeCl ₂ ·4H ₂ O	19.25	Spherical	20.32	Antibacterial activity/ Catalytic degradation	[42]
Green tea	Leaves	FeCl ₂ ·4H ₂ O/ FeCl ₃ ·6H ₂ O	85.44	Semi-spherical	9.4924	Antioxidant activity	[43]
<i>Aloe vera</i>	Leaves	FeCl ₂ ·4H ₂ O/FeCl ₃ ·6 H ₂ O	7.38	Semi-spherical	37.718	Antioxidant activity	[43]
Pine	Leaves	FeCl ₃ ·6H ₂ O	12–37	Spherical	N/A	Antibacterial/Anticancer activity	[44]
<i>Stevia rebaudiana Bertoni</i>	Leaves	Fe(NO ₃) ₃	20	spherical	5.35	Antioxidant activity	[45]
<i>Azardica indica</i>	Leaves	Fe(Cl) ₃ ·6H ₂ O / Fe(Cl) ₂ ·4H ₂ O	100	Spherical with few cubic NPs	13	Water treatment	[46]
<i>Cymbopogon citratus</i>	Leaves	Fe(Cl) ₃ ·6H ₂ O	9	Cubic shape	28	Environmental application	[47]
<i>Artemisia absinthium</i>	Leaves & stems	Fe(Cl) ₃ ·6H ₂ O/FeSO ₄ ·7H ₂ O	< 10	Spherical	N/A	Magnetic hyperthermia	[48]
<i>Garcinia mangostana</i>	Fruit peels	Fe(Cl) ₃ ·6H ₂ O/Fe(Cl) ₂ ·4H ₂ O	13.42	Spherical	73.15	Magnetic hyperthermia	[49]
<i>Gardenia resinifera</i>	Leaves	FeCl ₃ ·6H ₂ O	5	Spherical	8.5	Magnetic hyperthermia	[50]
<i>Pimenta dioica</i>	Leaves	Fe(Cl) ₃ ·6H ₂ O/Fe(Cl) ₂ ·4H ₂ O	15	Spherical	N/A	Photothermal therapy	[51]
<i>Punica granatum</i>	Fruit peels	Fe(Cl) ₃ ·6H ₂ O/Fe(Cl) ₂ ·4H ₂ O	14.38	Spherical	69	Magnetic resonance imaging (MRI)/Magnetic hyperthermia	[52]
<i>Psoralea corylifolia</i>	Seeds	Fe(Cl) ₃ ·6H ₂ O	39	Spherical	N/A	Anticancer activity	[53]
<i>Ceratonia siliqua</i>	Pericarps	Fe(Cl) ₃ ·6H ₂ O	7	Spherical	N/A	Amoxicillin degradation	[54]
<i>Phoenix dactylifera L.</i>	Leaves	Fe(Cl) ₃ ·6H ₂ O/Fe(Cl) ₂ ·4H ₂ O	20	Spherical	66.1	Antibacterial activity	[55]
<i>Phyllanthus niruri</i>	Leaves	(NH ₄) ₂ Fe(SO ₄)·2(H ₂ O) ₆ / NH ₄ Fe(SO ₄) ₂ ·12H ₂ O	10	Square	N/A	Antimicrobial activity	[56]
<i>Wedelia urticifolia</i>	Leaves	FeCl ₃	15–20	Rod-shape	N/A	Removal of dye-toxic material	[57]
<i>Mentha pulegium L.</i>	Leaves	FeCl ₃	22–34	Cubic shape	N/A	Photocatalysis	[58]
<i>Zanthoxylum armatum</i>	Leaves	FeCl ₃ /FeSO ₄	17	Spherical	128	Photocatalysis	[59]
<i>Lagenaria Siceraria</i>	Leaves	FeCl ₃ ·6H ₂ O	30–100	Cubic shape	N/A	Antimicrobial activity	[60]
<i>Andean blackberry</i>	Leaves	FeSO ₄ ·7H ₂ O	40–70	Spherical	N/A	Photocatalysis/Antioxidant	[61]
<i>Graptophyllum pictum</i>	Leaves	FeSO ₄ ·7H ₂ O	24	FCC shape	N/A	Targeted drug delivery	[62]
<i>Ficus hispida</i>	Leaves	FeSO ₄ ·7H ₂ O/FeCl ₃ ·6H ₂ O	10.96	Spherical	100	Photocatalysis	[63]
<i>Laurus nobilis</i>	Leaves	FeCl ₃ ·6H ₂ O	8.03	Hexagonal shape	N/A	Antifungal/Antibacterial activity	[20]
<i>Cydonia oblonga</i>	Seeds	Fe(Cl) ₃ ·6H ₂ O/Fe(Cl) ₂ ·4H ₂ O	50	Spherical	53	N/A	[64]
<i>Excoecaria cochinchinensis</i>	Leaves	FeCl ₃	20–30	Spherical	55	Removal of antibiotics	[65]
<i>Rubia tinctorum</i>	N/A	N/A	2–5	quasi-spherical	40.3	Catalysis	[66]

IONPs) compared with commercial IONPs (C-IONPs) [71]. Toxicity was assessed using embryonic and adult zebrafish models. P-IONPs demonstrated greater biocompatibility, with a higher LC₅₀ value at 72 h (202 ± 12 µg·mL⁻¹) than C-IONPs (126 ± 9 µg·mL⁻¹). The study found that physiological effects, such as lower hatching and heart rates, were more pronounced following C-IONP exposure, particularly

at concentrations of higher than 10 µg·mL⁻¹. Morphological abnormalities, including abnormal notochord and pericardial edema, were more severe in adult zebrafish with C-IONP at ≥20 µg·mL⁻¹, leading to significant lesions, belly bulging, and fin discoloration. These results underscore the enhanced safety profile of P-IONPs compared with C-IONPs, further supporting the use of plant-mediated synthesis

Table 3 Biocompatibility studies and cytotoxicity evaluation of green-synthesized iron oxide nanoparticles (IONPs).

Type of IONPs/IONPs-based materials	Plant used	Cell type	Toxicity test assay	Findings	References
Fe ₃ O ₄ Co Fe ₂ O ₄ Ne Fe ₂ O ₄	(<i>Aloe vera</i>) <i>Aloe barbadensis mill</i>	Murine hepatocellular carcinoma (Hepa1-6)	WST assay	Cell viability remained significantly high at approximately 80%, even under elevated concentrations of up to 0.1 µg·µL ⁻¹ . These findings substantiate the safety and compatibility of the ferrite materials at different concentrations. Moreover, the optical images indicate the absence of cellular apoptosis.	[72]
Fe ₃ O ₄ @γ-Fe ₂ O ₃	<i>Cinnamomum verum/Vanilla planifolia</i>	Immortalized brain microglia murine (BV-2)	N/A	The investigation evaluated the effects of green-synthesized IONPs on BV-2 cells at concentrations up to 100 µg·mL ⁻¹ . Notably, the IONPs demonstrated negligible cytotoxicity, with cell viability consistently exceeding 94% compared with control cells.	[73]
Fe ₃ O ₄	<i>Cardiospermum halicacabum</i>	Peripheral blood mononuclear cells (PBMCs)	MTT assay	The green-synthesized IONPs exhibited a cell viability of 84.04% ± 0.94% at a concentration of 100 µg·mL ⁻¹ on PBMCs. According to ISO 10993-5: 2009 standards, treatments are deemed nontoxic when cell viability exceeds 70%. Additionally, the mean IC50 value was determined to be 304.14 µg·mL ⁻¹ .	[71]
Fe ₃ O ₄	<i>Borassus flabellifer</i>	Murine fibroblasts (NIH/3T3)	MTT assay	After 24 h of exposure, cell viability fluctuated between 82% and 94% at all concentrations. After 48 h of incubation, cell viability varied from 86% to 95%. In every scenario, cell viability surpassed 80%, indicating the NPs' robust cytocompatibility with fibroblasts.	[74]
α-Fe ₂ O ₃	<i>Gardenia resiniferous</i>	Human mesenchymal cells (hMSCs)	Flow cytometry	After 24 and 48 h of incubation with green-synthesized IONPs, human mesenchymal cells exhibited cell viability 82% and 81%, respectively. This indicates a significant level of cell viability compared with the control, even at an elevated NP concentration of 1 mg·mL ⁻¹ .	[75]
Fe ₂ O ₃	<i>Artemisia absinthium</i>	Human keratinocytes (HaCaT)	Alamar Blue assay	Upon exposure to green-synthesized Fe ₂ O ₃ NPs, HaCaT viability remained largely unaffected, with no recorded reduction below 80% in the viable population.	[76]
Fe ₃ O ₄	<i>Nigella sativa</i>	Vero cells	MTT assay	The biogenic IONPs exhibited no discernible cytotoxic effects at the concentrations of 12.5, 25, 50, 100, and 200 µg·mL ⁻¹ for 48 h of exposure, thereby suggesting their biocompatibility.	[77]

for safer biomedical and environmental applications [71].

Biomedical Applications of IONPs

Due to the large surface area of IONPs, multiple functional groups can be attached to tumor-specific ligands, including monoclonal antibodies, peptides, or small molecules. This increases their utility in both diagnostic imaging and therapeutic drug delivery [77]. The magnetic properties of IONPs have numerous applications *in vivo*. IONPs can be used as magnetic CAs in MRI to diagnose benign or malignant tumors, as well as hyperthermia or thermoablation agents, where they are selectively heated by a high-frequency magnetic field [78].

Contrast agents for MRI

MRI is a commonly used noninvasive imaging technique for visualizing the interiors of living organisms. Along with positron emission

tomography, computed tomography, and ultrasound imaging, it is considered a primary imaging modality.

Mechanism of action of T1/T2 contrast agents

The radiofrequency signal of protons magnetized by an external magnetic field generates the MRI signal. These protons are primarily derived from water molecules. Radiofrequency pulses are used to excite magnetization, whereas magnetic field gradients are employed to facilitate spatial localization. MRI contrast reflects differences in signal intensity, which is influenced by factors, including the concentration of water molecules in the tissue, relaxation times (T1 and T2) of water protons, and mobility of water molecules (diffusion and flow) [79, 80]. MRI diagnostic accuracy can be significantly improved by using CAs that decrease the T1 or T2 relaxation times of water protons, thereby increasing image contrast [81–83]. T1 CAs increase the longitudinal relaxation time (T1) signal on T1-weighted imaging, resulting in a positive/brighter contrast enhancement, whereas T2 CAs decrease the T2 signal on T2-weighted imaging,

resulting in a negative/dark contrast enhancement. The effectiveness of MRI CAs in signal enhancement is determined by their relaxivity values (r_1 and r_2), which represent an increase in the relaxation rate resulting from the addition of 1 mmol/L CA. CA physicochemical properties, including its size, chemical structure, and accessibility of water molecules to its magnetic center, are crucial considerations in designing effective magnetic labels. The r_1 and r_2 values are crucial parameters influencing the effectiveness of MRI CAs and are essential for their successful implementation in clinical and research settings [84].

Gadolinium-based contrast agents (GBCAs)

GBCAs effectively enhance MRI contrast, but they are associated with significant adverse effects. They have been linked to the development of nephrogenic systemic fibrosis (NSF), a condition that can cause fibrotic skin contractures and, in severe cases, even fractures or mortality [83–86]. Reportedly, these complexes of heavy metals can induce brain lesions, which may be exacerbated in individuals with liver or kidney impairments because of their diminished capacity to eliminate GBCAs from the body [87, 88]. Furthermore, the problems associated with GBCA toxicity are worsened by the fact that they have a brief half-life in the bloodstream [89, 90]. This necessitates that patients receive multiple contrast administrations to obtain the requisite images, underscoring the pressing need for a more biocompatible T1 CA.

IONPs as CAs

IONPs have received extensive attention as CAs for MRI due to their superior magnetic properties, such as superparamagnetism, which leads to enhanced relaxivity, and their biocompatibility, attributed to their integration into iron metabolism. Additionally, IONP surfaces can be easily functionalized with target molecules, making them ideal for molecular

imaging applications [91]. The mechanism by which IONPs function as CAs for T1- and/or T2-weighted MRI involves the interaction of the body's hydrogen nuclei with a strong magnetic field in an MRI scanner. When a radiofrequency pulse is applied, the magnetization from the hydrogen nuclei interacts with the receiver coil, allowing spin polarization to be detected. Upon pulse removal, the magnetization returns to its equilibrium position, resulting in T1 relaxation or T2 decay. The T1 and/or T2 relaxation times vary with the number of water protons in different organs, creating contrast in the MR images. After oral or intravenous administration, IONPs can decrease the T1 and/or T2 relaxation times of water protons in various organs, thereby producing contrast in MR images. [92–95].

Green-synthesized IONPs as CAs

IONPs produced via GS provide safer profiles than chemically synthesized CAs [96–102]. Although some studies have demonstrated the potential of biosynthesized IONPs as MRI CAs (Table 4), these agents are typically considered to be T2-weighted and less efficient than T1 CAs [83]. The available literature on the use of biosynthesized IONPs as MRI CAs is relatively scarce. Further research is required to investigate the potential of these green-synthesized IONPs for MRI contrast applications. Moreover, most of the existing studies have focused on the use of IONPs as T2-weighted CAs, and the production of IONPs as T1-weighted CAs requires further exploration.

Surface modification of IONPs for MRI

The enhancement of MRI contrast efficacy can be achieved by modifying the IONP surface. For instance, Illes et al. demonstrated that the attachment of polyethylene glycol (PEG) moieties to IONPs enhances their compatibility with biological systems. Moreover, this functionalization significantly increased the r_2 relaxivity parameter, reaching a value

Table 4 Previous relaxometry studies investigating the MRI contrast properties of green-synthesized IONPs using plant parts.

Plant name	Magnetic field strength	Relaxivity (r_1)	Relaxivity (r_2)	Ref.
<i>Punica granatum</i>				
S1	3 T	1 mL· $\mu\text{g}^{-1}\cdot\text{s}^{-1}$	N/A	[101]
S2		0.62 mL· $\mu\text{g}^{-1}\cdot\text{s}^{-1}$		
S3		0.39 mL· $\mu\text{g}^{-1}\cdot\text{s}^{-1}$		
<i>Pimenta dioica</i>	1.5 T	10.67 mM $^{-1}\cdot\text{s}^{-1}$	140.87 mM $^{-1}\cdot\text{s}^{-1}$	[52]
<i>Citrus aurantium</i>	1.5 T	19.4 ± 0.3 mM $^{-1}\cdot\text{s}^{-1}$	185.8 ± 9.3 mM $^{-1}\cdot\text{s}^{-1}$	[102]

of $451 \text{ mM}^{-1}\cdot\text{s}^{-1}$. This magnitude of relaxivity is one of the highest among the existing data concerning core-shell magnetite NPs. Furthermore, the investigation revealed that the PEG-modified IONPs exhibited a notable absence of unspecific adherence to cellular entities. This absence of cell interaction or internalization facilitates the circulation of the magnetic NPs within the vascular network during MRI [98]. Additionally, Lazaro-Carillo et al. conducted a comparative analysis involving IONPs coated with PEG and Ferumoxytol, an FDA-approved pharmaceutical agent. It was found that the PEG-coated IONPs exhibited r_2 relaxivity of $189.94 \text{ mM}^{-1}\cdot\text{s}^{-1}$. Remarkably, this value surpassed the r_2 relaxivity of Ferumoxytol-coated IONPs, which was $81 \text{ mM}^{-1}\cdot\text{s}^{-1}$ [103]. An alternative approach involves the application of naturally occurring polymers to coat IONPs, thereby augmenting their physicochemical attributes and biocompatibility. Among the types of available natural polymers, chitosan has garnered notable attention owing to its multifaceted biological characteristics, including biocompatibility, biodegradability, non-toxicity, and inherent bioactivity. Khmara et al. demonstrated that IONPs with chitosan exhibited an r_2 relaxivity of $238.16 \text{ mM}^{-1}\cdot\text{s}^{-1}$. Notably, this nanoformulation exhibited the potential to function as a negative MRI CA. This conclusion arises from the observed excellent relaxivity value compared with established iron-based CAs used in clinical settings, specifically Feridex ($r_2 = 120 \text{ mM}^{-1}\cdot\text{s}^{-1}$), Resovist ($r_2 = 186 \text{ mM}^{-1}\cdot\text{s}^{-1}$), and Combidex ($r_2 = 65 \text{ mM}^{-1}\cdot\text{s}^{-1}$) [100].

Magnetic hyperthermia

Local hyperthermia, a method for treating cancer, has proven ineffective for treating severe forms of cancer due to inherent limitations, including uneven

temperature distribution within the tumor and the inability to regulate overheating in deep-seated regions of the mass. Therefore, it is essential to develop a novel technique capable of effectively addressing previously addressed obstacles [103, 104]. Nano-magnetic hyperthermia (NMH) has been established as an innovative approach for eradicating malignant tumors by using the hyperthermic effects of IONPs. The primary advantage of NMH is attributed to the capacity of IONPs to penetrate remote regions and create differential temperature profiles between healthy tissues and the tumor [105]. As magnetic NPs, IONPs have garnered recognition as superior candidates for hyperthermia therapy due to their unique attributes, including the ability to eliminate cancerous cells via magnetically induced heating [104]. Moreover, MH using IONPs has significant promise in preclinical studies for treating various cancer types, including breast cancer, glioblastoma, and prostate cancer. These studies typically involve the intravenous injection of IONPs, which localize at tumor sites and generate localized heat ($41\text{--}46 \text{ }^\circ\text{C}$) upon exposure to an alternating magnetic field, effectively inducing tumor cell death while sparing healthy tissues. Clinical trials, like those by MagForce AG for glioblastoma, have demonstrated the safety and efficacy of this approach, with direct injection of IONPs into tumors followed by magnetic field exposure [106, 107]. Additionally, ongoing trials for advanced prostate cancer are exploring similar approaches, highlighting the versatility of IONPs in various cancer types. However, challenges remain in optimizing nanoparticle distribution and minimizing collateral damage to surrounding tissues, as evidenced by the need for precise coil configurations to reduce eddy currents [108]. Overall, MH represents a promising

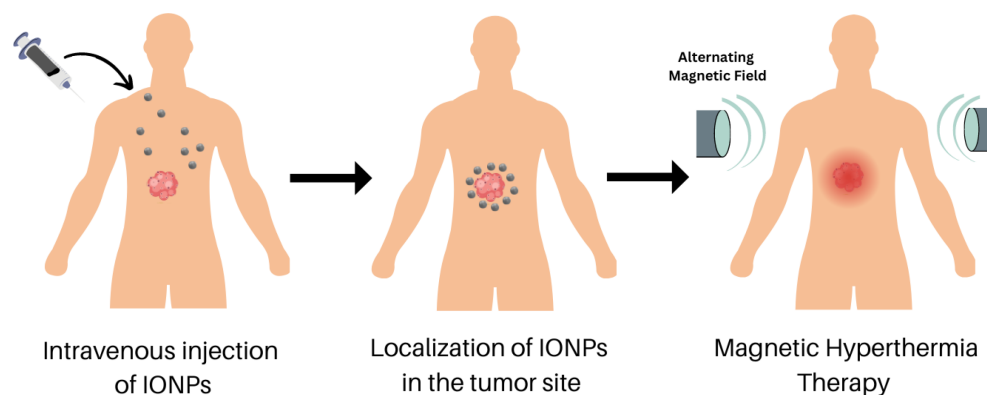


Fig. 5 Illustration of the mechanism of magnetic hyperthermia when IONPs are injected intravenously into a human body.

adjunctive therapy for cancer treatment, warranting further investigation and refinement [109].

Mechanism of IONPs in magnetic hyperthermia

In MH, IONPs are exposed to an alternating-current magnetic field. As the NPs oscillate in response to the applied field, energy is lost and converted to heat, leading to hyperthermia, as illustrated in Fig. 5. Neel relaxation, which is the fluctuation of the magnetic moment of NPs over an anisotropic energy barrier, and Brown relaxation, which is the energy loss due to viscous particle reorientation in solution, are two distinct types of energy dissipation contributing to MH [110]. The specific absorption rate (SAR) represents the heating power per unit mass of a dissipating material and is used to quantify the heating capacity of magnetic NPs [111].

Heat application affects MH outcome. A moderate amount of heat, approximately 40 °C, can disrupt the structure of cellular components, including phospholipids, proteins, and nucleic acids, thereby impairing their functions and causing cell death. At temperatures higher than 45 °C, proteins denature and are destroyed by heat. Surprisingly, cell damage has been observed without a significantly increased temperature [109, 110]. Additionally, MH increases the production of reactive oxygen species, contributing to the cytotoxic effect [111–113]. Furthermore, tissue-level MH reportedly improves oxygenation in cancer cells, thereby increasing radiosensitivity. Due to its biological effects, it is highly likely that combining MH with other

treatments will produce favorable outcomes [99].

Green-synthesized IONPs in magnetic hyperthermia

As previously mentioned, the GS method for producing IONPs offers multiple advantages, including environmental friendliness, cost-effectiveness, and the generation of IONPs with diverse sizes and shapes suitable for various applications, such as hyperthermia therapy. This method also uses fewer toxic substances and organic solvents while protecting NPs from oxidation and aggregation [114]. Consequently, numerous studies have been conducted to develop IONPs using plants as a reducing, capping, and stabilizing agent for the hyperthermia treatment of cancer. In 2017, Horst et al. reported the highest measured SAR for IONPs containing gum Arabic as a reducing agent, reaching 218 W·g⁻¹ [115]. This result was obtained under specific conditions of 260-kHz frequency and 52-kA·m⁻¹ field amplitude. The high SAR value suggests that iron oxide can be used in hyperthermia treatment. Hermosa et al. used *Aloe vera* in IONP synthesis and reported a SAR value of 101 W·g⁻¹ with a saturation magnetization of 52 emu·g⁻¹ [72]. Additionally, the study discovered that the cell survival rate following exposure to iron oxide synthesized using *Aloe vera* remained high, even at concentrations of 0.1 g·L⁻¹, indicating the material's biocompatibility and safety. Therefore, the iron oxide synthesized with *Aloe vera* may be suitable for applications such as drug delivery systems and hyperthermia without endangering the bodily tissues. Additional studies are reported in Table 5.

Table 5 Previous magnetic hyperthermia (MH) studies on green-synthesized iron oxide nanoparticles (IONPs) using different plant extracts.

Plants	Frequency of magnetic field (kHz)	Alternating magnetic field strength (AMF) (kA·m ⁻¹)	Saturation magnetization (M_0) (emu·g ⁻¹)	Hyperthermia temperature (T_{IH}) (°C)	Specific absorption rate (SAR) (W·g ⁻¹)	Ref.
<i>Gum arabia</i>	260	52.00	44.20	N/A	218.00	[115]
<i>Aloe vera</i>	60	N/A	52.00	N/A	101.00	[72]
	318	23.60		45	196.95	
<i>Punica granatum</i>	313	31.50	48.00	47	212.56	[21]
	312	39.37		48	232.29	
	318	23.60		42	98.74	
<i>Garcinia mangostana</i>	313	31.50	69.42	43	130.48	[55]
	312	39.37		44	179.85	
<i>Cinnamomun verum</i>	570	23.90	70.84	N/A	335.69	[73]
<i>Vanilla planifolia</i>	570	23.90	60.00	N/A	233.96	[73]

N/A: not available

Current research on the GS of IONPs for use in MH is insufficient, necessitating additional studies to fill the existing knowledge gap. Several studies have investigated IONP synthesis using eco-friendly techniques, but few have examined its efficacy in hyperthermia applications. The effectiveness of these NPs in MH, and their biocompatibility and potential toxicity, requires further investigation. Such research could provide valuable insights into the suitability of GS techniques for producing NPs for biomedical applications.

Surface modification of IONPs for magnetic hyperthermia

Surface modification of magnetic NPs can enhance their specific loss power (SLP), which refers to their ability to dissipate heat. By mitigating agglomeration, these surface alterations can influence local magnetostatic interactions. Alkhayal et al. investigated the use of PEG to functionalize Fe₃O₄/rGO NPs as a potential MH agent. They found that the application of PEG coating played a crucial role in enhancing NP stability, thereby effectively mitigating their tendency toward aggregation. Moreover, the absence of PEG coating in the nanocomposites led to lower magnetic heating efficiency [116]. Furthermore, Gharibkandi reported that the introduction of PEG into a composite comprising IONPs and gold (Au) yielded a notable outcome. This augmentation facilitated the rapid achievement of the heating required for cellular apoptosis and necrosis. Consequently, this modification significantly enhanced the efficacy of the nanocomposite as a hyperthermia-inducing agent [117].

Vassallo et al. functionalized IONPs using sodium citrate, significantly enhancing their heating efficiency and colloidal stability [118]. Specifically, the sodium citrate coating resulted in a 2-fold increase in SLP, achieving approximately 170 W·g⁻¹ under a magnetic field of 100 kHz and 48 kA·m⁻¹, while ensuring improved dispersion and prolonged stability in solution [118]. Furthermore, Rajan et al. reported that IONPs coated with glutamic acid exhibited increased anisotropy, elevated magnetic susceptibility, a quicker relaxation time, and an SAR value of 130 W·g⁻¹, suggesting their potential stability for clinical MH [119]. In another study by Gonçalves et al., IONPs were surface-modified with fucoidan, a marine algae-derived sulfated polysaccharide. The

SLP value for these fucoidan-modified IONPs was 130 W·g⁻¹. Additionally, previous studies have indicated the anticancer potential of fucoidan, demonstrating its ability to diminish tumor dimensions [120]. There is also evidence suggesting its synergistic efficacy when combined with other therapeutic methods, such as photothermal therapy [121].

Challenges and Conclusions

Nanotechnology has become an increasingly popular field of study in recent years. Contributing to this increase are metal oxides, particularly IONPs, owing to their unique properties and applications. This study investigated various aspects of IONPs, including their synthesis, characterization, cytotoxicity, and biomedical applications. Traditional chemical and physical methods for synthesizing NPs have disadvantages, such as toxicity and high cost. The green-synthesized IONPs provides an economical and eco-friendly alternative. Moreover, their low toxicity and scalability make GS techniques increasingly popular. Various techniques for characterizing IONPs have been used to investigate their properties, significantly elucidating their physical, chemical, and magnetic characteristics. Furthermore, the evaluation of the cytotoxicity of green-synthesized IONPs in this study confirmed their biocompatibility, making them suitable for biomedical applications. Due to their magnetic properties, IONPs have been used as CAs in MRI, making them particularly advantageous for imaging purposes, as they can be used to detect and visualize cancer cells. IONPs have also been studied for their use in MH, a promising cancer treatment technique. This method uses the magnetic properties of IONPs to generate heat under the influence of an external magnetic field, which can eliminate cancer cells. To fully harness the potential of IONPs for MH and MRI contrast applications, it is imperative to investigate environmentally friendly synthesis methods. The relationship between particle size and its inherent magnetic properties, which influence MH and MRI applications, remains underexplored. Additionally, a comprehensive experimental design method for optimizing the synthesis and functionalization of IONPs is essential. Developing such a method would allow for precise control over the size, shape, and surface properties of IONPs,

significantly enhancing their performance in biomedical applications. A noticeable gap exists in the literature concerning optimizing the synthesis and functionalization strategies through a comprehensive design of experiments approach. Furthermore, the connection between synthesis parameters and the resulting magnetic attributes of IONPs remains poorly understood. Addressing these research gaps would provide invaluable insights and directions for future investigations in this field. With additional research and development, IONPs could play even greater roles in disease diagnosis and treatment, improving patient outcomes and quality of life.

CRedit Author Statement

Mohamed Abdelmonem, Romesa Soomro, and Mohamed Ahmed Ibrahim: conceptualization, writing–review, editing, and visualization. **Emma Ziezie Tarmizie, Norazalina Saad:** project administration. **Che Azurahaman Che Abdullah, Kim Wei Chan:** validation and supervision.

Acknowledgements

The authors sincerely appreciate Universiti Putra Malaysia for providing essential technical support and access to subscription databases.

Conflict of Interests

The authors declare that there is no conflict of interest regarding the publication of this paper.

References

- [1] N.B. Turan, H.S. Erkan, G.O. Engin, et al. Nanoparticles in the aquatic environment: Usage, properties, transformation and toxicity—a review. *Process Safety and Environmental Protection*, 2019, 130: 238–249. <https://doi.org/10.1016/j.psep.2019.08.014>
- [2] S. Vasantharaj, S. Sathiyavimal, P. Senthilkumar, et al. Biosynthesis of iron oxide nanoparticles using leaf extract of *Ruellia tuberosa*: Antimicrobial properties and their applications in photocatalytic degradation. *Journal of Photochemistry and Photobiology B: Biology*, 2019, 192: 74–82. <https://doi.org/10.1016/j.jphotobiol.2018.12.025>
- [3] T.A. Saleh, G. Fadillah, O.A. Saputra. Nanoparticles as components of electrochemical sensing platforms for the detection of petroleum pollutants: A review. *TrAC Trends in Analytical Chemistry*, 2019, 118: 194–206. <https://doi.org/10.1016/j.trac.2019.05.045>
- [4] M. Hussain, N.I. Raja, M. Iqbal, et al. Applications of plant flavonoids in the green synthesis of colloidal silver nanoparticles and impacts on human health. *Iranian Journal of Science and Technology, Transactions A: Science*, 2019, 43(3): 1381–1392. <https://doi.org/10.1007/s40995-017-0431-6>
- [5] A. Arya, V. Mishra, T.S. Chundawat. Green synthesis of silver nanoparticles from green algae (*Botryococcus braunii*) and its catalytic behavior for the synthesis of benzimidazoles. *Chemical Data Collections*, 2019, 20: 100190. <https://doi.org/10.1016/j.cdc.2019.100190>
- [6] N. Pantidos. Biological synthesis of metallic nanoparticles by bacteria, fungi and plants. *Journal of Nanomedicine & Nanotechnology*, 2014, 5(5): 1000233. <https://doi.org/10.4172/2157-7439.1000233>
- [7] S.H. Chen, R. Yuan, Y.Q. Chai, et al. Electrochemical sensing of hydrogen peroxide using metal nanoparticles: A review. *Microchimica Acta*, 2013, 180(1): 15–32. <https://doi.org/10.1007/s00604-012-0904-4>
- [8] A. Rastar, M.E. Yazdanshenas, A. Rashidi, et al. Theoretical Review of Optical Properties of Nanoparticles. *Journal of Engineered Fibers and Fabrics*, 2013, 8(2): 155892501300800220. <https://doi.org/10.1177/155892501300800221>
- [9] E.A. Campos, D.V.B.S. Pinto, J.I.S. de Oliveira, et al. Synthesis, characterization and applications of iron oxide nanoparticles - A short review. *Journal of Aerospace Technology and Management*, 2015, 7(3): jul./Sep.2015. <https://doi.org/10.5028/jatm.v7i3.471>
- [10] S. Mourdikoudis, R.M. Pallares, N.T.K. Thanh. Characterization techniques for nanoparticles: Comparison and complementarity upon studying nanoparticle properties. *Nanoscale*, 2018, 10(27): 12871–12934. <https://doi.org/10.1039/c8nr02278j>
- [11] S.K. Srikar, D.D. Giri, D.B. Pal, et al. Green synthesis of silver nanoparticles: A review. *Green and Sustainable Chemistry*, 2016, 6(1): 34–56. <https://doi.org/10.4236/gsc.2016.61004>
- [12] M. Abdelmonem, E.L. Albert, A. Norman, et al. Surface functionalization of 2D MOs for enhanced biocompatibility and biomedical applications. In: *Emerging Applications of Novel Nanoparticles*. Cham: Springer, 2024: 175–198. https://doi.org/10.1007/978-3-031-57843-4_7
- [13] S.P. Patil, R.Y. Chaudhari, M.S. Nemade. *Azadirachta indica* leaves mediated green synthesis of metal oxide nanoparticles: A review. *Talanta Open*, 2022, 5: 100083. <https://doi.org/10.1016/j.talo.2022.100083>
- [14] M. Abdelmonem, E.L. Albert, M.A. Alhadad, et al. Plant-polyphenol-mediated synthesis of magnetic biocompatible iron oxide nanoparticles for diagnostic imaging and management of neurodegenerative diseases. *Precision Nanomedicine*, 2024, 7(1): 1233–1251. <https://doi.org/10.33218/001c.92424>
- [15] A. Rajan, N.K. Sahu. Review on magnetic nanoparticle-mediated hyperthermia for cancer therapy. *Journal of Nanoparticle Research*, 2020, 22: 319. <https://doi.org/10.1007/s11051-020-05045-9>
- [16] A.G. Roca, L. Gutiérrez, H. Gavilán, et al. Design strategies for shape-controlled magnetic iron oxide nanoparticles. *Advanced Drug Delivery Reviews*, 2019, 138: 68–104. <https://doi.org/10.1016/j.addr.2018.12.008>
- [17] Y. Sun, S.K. Gray, S. Peng. Surface chemistry: a non-negligible parameter in determining optical properties of small colloidal metal nanoparticles. *Physical Chemistry Chemical Physics*, 2011, 13(25): 11814–11826. <https://doi.org/10.1039/c1cp20265k>
- [18] M. Yusefi, K. Shamel, R.R. Ali, et al. Evaluating anticancer activity of plant-mediated synthesized iron oxide nanoparticles using punica granatum fruit peel

- extract. *Journal of Molecular Structure*, 2020, 1204: 127539. <https://doi.org/10.1016/j.molstruc.2019.127539>
- [19] W.S. Mohamed, N.M.A. Hadia, B. Al bakheet, et al. Impact of Cu²⁺ cations substitution on structural, morphological, optical and magnetic properties of Co_{1-x}Cu_xFe₂O₄ nanoparticles synthesized by a facile hydrothermal approach. *Solid State Sciences*, 2022, 125: 106841. <https://doi.org/10.1016/j.solidstatesciences.2022.106841>
- [20] M. Jamzad, M. Kamari Bidkorpeh. Green synthesis of iron oxide nanoparticles by the aqueous extract of *Laurus nobilis* L. leaves and evaluation of the antimicrobial activity. *Journal of Nanostructure in Chemistry*, 2020, 10(3): 193–201. <https://doi.org/10.1007/s40097-020-00341-1>
- [21] S. Dutta, S. Parida, C. Maiti, et al. Polymer grafted magnetic nanoparticles for delivery of anticancer drug at lower pH and elevated temperature. *Journal of Colloid and Interface Science*, 2016, 467: 70–80. <https://doi.org/10.1016/j.jcis.2016.01.008>
- [22] A. Zengin, U. Tamer, T. Caykara. Synthesis of superparamagnetic and thermoresponsive hybrid nanoparticles via surface-mediated RAFT polymerization of di(ethylene glycol) ethyl ether acrylate and (oligoethylene glycol) methyl ether acrylate. *Journal of Polymer Science Part A: Polymer Chemistry*, 2013, 51(16): 3420–3428. <https://doi.org/10.1002/pola.26739>
- [23] M. Razavi, E. Salahinejad, M. Fahmy, et al. Green chemical and biological synthesis of nanoparticles and their biomedical applications. In: *Green Processes for Nanotechnology*. Cham: Springer International Publishing, 2015: 207–235. https://doi.org/10.1007/978-3-319-15461-9_7
- [24] M. Abdelmonem, E.L. Albert, N.K.R. Zainon, et al. Biosynthesis of iron oxide nanoparticles (IONPs): Toxicity evaluation and applications for magnetic resonance imaging and magnetic hyperthermia. In: *Lecture Notes in Nanoscale Science and Technology*. S. Anil Bansal, V. Khanna, N. Balakrishnan, et al. eds. Cham: Springer Nature Switzerland, 2024: 229–249. https://doi.org/10.1007/978-3-031-57843-4_9
- [25] N. Abid, A.M. Khan, S. Shujait, et al. Synthesis of nanomaterials using various top-down and bottom-up approaches, influencing factors, advantages, and disadvantages: A review. *Advances in Colloid and Interface Science*, 2022, 300: 102597. <https://doi.org/10.1016/j.cis.2021.102597>
- [26] A. Demirbas, T. Karaytuğ, N. Arabaci, et al. Synthesis of metallic and metal oxide nanomaterials. In: *Green Synthesis of Nanomaterials for Bioenergy Applications*. N. Srivastava, M. Srivastava, P.K. Mishra, et al. eds. John Wiley & Sons Ltd., 2020: 99–123. <https://doi.org/10.1002/9781119576785.ch4>
- [27] S. Anu Mary Ealia, M.P. Saravanakumar. A review on the classification, characterisation, synthesis of nanoparticles and their application. *IOP Conference Series: Materials Science and Engineering*, 2017, 263: 032019. <https://doi.org/10.1088/1757-899x/263/3/032019>
- [28] S.X. Liu, B. Yu, S. Wang, et al. Preparation, surface functionalization and application of Fe₃O₄ magnetic nanoparticles. *Advances in Colloid and Interface Science*, 2020, 281: 102165. <https://doi.org/10.1016/j.cis.2020.102165>
- [29] M.C. Sportelli, M. Izzi, A. Volpe, et al. The pros and cons of the use of laser ablation synthesis for the production of silver nano-antimicrobials. *Antibiotics*, 2018, 7(3): 67. <https://doi.org/10.3390/antibiotics7030067>
- [30] S. Shahidi, B. Moazzenchi, M. Ghoranneviss. A review-application of physical vapor deposition (PVD) and related methods in the textile industry. *The European Physical Journal Applied Physics*, 2015, 71(3): 31302. <https://doi.org/10.1051/epjap/2015140439>
- [31] I. Sayago, E. Hontañón, M. Aleixandre. Preparation of tin oxide nanostructures by chemical vapor deposition. In: *Tin Oxide Materials*. Amsterdam: Elsevier, 2020: 247–280. <https://doi.org/10.1016/b978-0-12-815924-8.00009-8>
- [32] P.G. Jamkhande, N.W. Ghule, A.H. Bamer, et al. Metal nanoparticles synthesis: An overview on methods of preparation, advantages and disadvantages, and applications. *Journal of Drug Delivery Science and Technology*, 2019, 53: 101174. <https://doi.org/10.1016/j.jddst.2019.101174>
- [33] H.Y. Li, B.S. Yang. Model evaluation of particle breakage facilitated process intensification for Mixed-Suspension-Mixed-Product-Removal (MSMPR) crystallization. *Chemical Engineering Science*, 2019, 207: 1175–1186. <https://doi.org/10.1016/j.ces.2019.07.030>
- [34] N. Baig, I. Kammakam, W. Falath. Nanomaterials: A review of synthesis methods, properties, recent progress, and challenges. *Materials Advances*, 2021, 2(6): 1821–1871. <https://doi.org/10.1039/d0ma00807a>
- [35] O.P. Bolade, A.B. Williams, N.U. Benson. Green synthesis of iron-based nanomaterials for environmental remediation: A review. *Environmental Nanotechnology, Monitoring & Management*, 2020, 13: 100279. <https://doi.org/10.1016/j.enmm.2019.100279>
- [36] M. Herlekar, S. Barve, R. Kumar. Plant-mediated green synthesis of iron nanoparticles. *Journal of Nanoparticles*, 2014, 2014: 140614. <https://doi.org/10.1155/2014/140614>
- [37] Jayakumari. Phytochemicals and pharmaceutical: Overview. In: *Advances in Pharmaceutical Biotechnology*. Singapore: Springer Singapore, 2020: 163–173. https://doi.org/10.1007/978-981-15-2195-9_14
- [38] M. Nasrollahzadeh, M. Atarod, M. Sajjadi, et al. Plant-mediated green synthesis of nanostructures: Mechanisms, characterization, and applications. In: *Interface Science and Technology*. Amsterdam: Elsevier, 2019: 199–322. <https://doi.org/10.1016/b978-0-12-813586-0.00006-7>
- [39] L.L. Huang, X.L. Weng, Z.L. Chen, et al. Green synthesis of iron nanoparticles by various tea extracts: Comparative study of the reactivity. *Spectrochimica Acta Part A: Molecular and Biomolecular Spectroscopy*, 2014, 130: 295–301. <https://doi.org/10.1016/j.saa.2014.04.037>
- [40] P. Somchaidee, K. Tedsree. Green synthesis of high dispersion and narrow size distribution of zero-valent iron nanoparticles using guava leaf (*Psidium guajava* L.) extract. *Advances in Natural Sciences: Nanoscience and Nanotechnology*, 2018, 9(3): 035006. <https://doi.org/10.1088/2043-6254/aad5d7>
- [41] S. Lakshminarayanan, M.F. Shereen, K.L. Niraimathi, et al. Author Correction: One-pot green synthesis of iron oxide nanoparticles from *Bauhinia tomentosa*: Characterization and application towards synthesis of 1, 3 diolein. *Scientific Reports*, 2021, 11: 17707. <https://doi.org/10.1038/s41598-021-87960-y>
- [42] C. Sudhakar, M. Poonkothai, T. Selvankumar, et al. Biomimetic synthesis of iron oxide nanoparticles using *Canthium coromandelicum* leaf extract and its antibacterial and catalytic degradation of Janus green. *Inorganic Chemistry Communications*, 2021, 133: 108977. <https://doi.org/10.1016/j.inoche.2021.108977>
- [43] N. Mohamed, O.E.A. Hessen, H.S. Mohammed.

- Thermal stability, paramagnetic properties, morphology and antioxidant activity of iron oxide nanoparticles synthesized by chemical and green methods. *Inorganic Chemistry Communications*, 2021, 128: 108572. <https://doi.org/10.1016/j.inoche.2021.108572>
- [44] M.R. Parsaeian, A.M. Haji Shabani, S. Dadfarnia, et al. Evaluating the biological activities of functionalized magnetic iron oxide nanoparticles with different concentrations of aqueous pine leaves extract. *Journal of the Indian Chemical Society*, 2022, 99(10): 100707. <https://doi.org/10.1016/j.jics.2022.100707>
- [45] M. Khatami, H.Q. Alijani, B. Fakheri, et al. Superparamagnetic iron oxide nanoparticles (SPIONs): Greener synthesis using Stevia plant and evaluation of its antioxidant properties. *Journal of Cleaner Production*, 2019, 208: 1171–1177. <https://doi.org/10.1016/j.jclepro.2018.10.182>
- [46] Y.W. Getahun, J. Gardea-Torresdey, F.S. Manciu, et al. A. Green synthesized superparamagnetic iron oxide nanoparticles for water treatment with alternative recyclability. *Journal of Molecular Liquids*, 2022, 356: 118983. <https://doi.org/10.1016/j.molliq.2022.118983>
- [47] D. Patiño-Ruiz, L. Sánchez-Botero, L. Tejada-Benitez, et al. Green synthesis of iron oxide nanoparticles using Cymbopogon citratus extract and sodium carbonate salt: Nanotoxicological considerations for potential environmental applications. *Environmental Nanotechnology, Monitoring & Management*, 2020, 14: 100377. <https://doi.org/10.1016/j.enmm.2020.100377>
- [48] E.A. Moacă, V. Socoliuc, D. Stoian, et al. Synthesis and characterization of bioactive magnetic nanoparticles from the perspective of hyperthermia applications. *Magnetochemistry*, 2022, 8(11): 145. <https://doi.org/10.3390/magnetochemistry8110145>
- [49] M. Yusefi, K. Shameli, O. Su Yee, et al. Green synthesis of Fe₃O₄ nanoparticles stabilized by a garcinia mangostana fruit peel extract for hyperthermia and anticancer activities. *International Journal of Nanomedicine*, 2021, 16: 2515–2532. <https://doi.org/10.2147/ijn.s284134>
- [50] V.C. Karade, S.B. Parit, V.V. Dawkar, et al. A green approach for the synthesis of α -Fe₂O₃ nanoparticles from Gardenia resinifera plant and its *in vitro* hyperthermia application. *Heliyon*, 2019, 5(7): e02044. <https://doi.org/10.1016/j.heliyon.2019.e02044>
- [51] P. Kharey, S.B. Dutta, M. Manikandan, et al. Green synthesis of near-infrared absorbing eugenate capped iron oxide nanoparticles for photothermal application. *Nanotechnology*, 2020, 31(9): 095705. <https://doi.org/10.1088/1361-6528/ab56b6>
- [52] M. Yusefi, K. Shameli, Z. Hedayatnasab, et al. Green synthesis of Fe₃O₄ nanoparticles for hyperthermia, magnetic resonance imaging and 5-fluorouracil carrier in potential colorectal cancer treatment. *Research on Chemical Intermediates*, 2021, 47(5): 1789–1808. <https://doi.org/10.1007/s11164-020-04388-1>
- [53] P.C. Nagajyothi, M. Pandurangan, D.H. Kim, et al. Green synthesis of iron oxide nanoparticles and their catalytic and *in vitro* anticancer activities. *Journal of Cluster Science*, 2017, 28(1): 245–257. <https://doi.org/10.1007/s10876-016-1082-z>
- [54] D. Aksu Demirezen, Y.Ş. Yıldız, D. Demirezen Yılmaz. Amoxicillin degradation using green synthesized iron oxide nanoparticles: Kinetics and mechanism analysis. *Environmental Nanotechnology, Monitoring & Management*, 2019, 11: 100219. <https://doi.org/10.1016/j.enmm.2019.100219>
- [55] A. Majid, F. Naz, H. Ali Jamro, et al. Facile green synthesis of iron oxide nanoparticles using phoenix dactylifera L. seed extract and their antibacterial applications. *Journal of Pharmaceutical Research International*, 2021: 21–29. <https://doi.org/10.9734/jpri/2021/v33i26b31478>
- [56] V.G. Viju Kumar, A.A. Prem. Green synthesis and characterization of iron oxide nanoparticles using phyllanthus niruri extract. *Oriental Journal of Chemistry*, 2018, 34(5): 2583–2589. <https://doi.org/10.13005/ojc/340547>
- [57] M.Y. Rather, S. Sundarapandian. Magnetic iron oxide nanorod synthesis by *Wedelia urticifolia* (Blume) DC. leaf extract for methylene blue dye degradation. *Applied Nanoscience*, 2020, 10(7): 2219–2227. <https://doi.org/10.1007/s13204-020-01366-2>
- [58] A. Bouafia, S.E. Laouini. Green synthesis of iron oxide nanoparticles by aqueous leaves extract of Mentha Pulegium L.: Effect of ferric chloride concentration on the type of product. *Materials Letters*, 2020, 265: 127364. <https://doi.org/10.1016/j.matlet.2020.127364>
- [59] A.V. Ramesh, D. Rama Devi, S. Mohan Botsa, et al. Facile green synthesis of Fe₃O₄ nanoparticles using aqueous leaf extract of *Zanthoxylum armatum* DC. for efficient adsorption of methylene blue. *Journal of Asian Ceramic Societies*, 2018, 6(2): 145–155. <https://doi.org/10.1080/21870764.2018.1459335>
- [60] S. Kanagasubbulakshmi, K. Kadirvelu. Green synthesis of iron oxide nanoparticles using Lageneria siceraria and evaluation of its Antimicrobial activity. *Defence Life Science Journal*, 2017, 2(4): 422. <https://doi.org/10.14429/dlsj.2.12277>
- [61] B. Kumar, K. Smita, L. Cumbal, et al. Phytosynthesis and photocatalytic activity of magnetite (Fe₃O₄) nanoparticles using the Andean blackberry leaf. *Materials Chemistry and Physics*, 2016, 179: 310–315. <https://doi.org/10.1016/j.matchemphys.2016.05.045>
- [62] I.P. Sari, Y. Yulizar. Green synthesis of magnetite (Fe₃O₄) nanoparticles using *Graptophyllum pictum* leaf aqueous extract. *IOP Conference Series: Materials Science and Engineering*, 2017, 191: 012014. <https://doi.org/10.1088/1757-899x/191/1/012014>
- [63] A.V. Ramesh, B. Lavakusa, B.S. Mohan, et al. A facile plant mediated synthesis of magnetite nanoparticles using aqueous leaf extract of ficus hispida L. for adsorption of organic dye. *IOSR Journal of Applied Chemistry*, 2017, 10(7): 35–43. <https://doi.org/10.9790/5736-1007013543>
- [64] R. Rahmani, M. Gharanfoli, M. Gholamin, et al. Green synthesis of 99mTc-labeled-Fe₃O₄ nanoparticles using Quince seeds extract and evaluation of their cytotoxicity and biodistribution in rats. *Journal of Molecular Structure*, 2019, 1196: 394–402. <https://doi.org/10.1016/j.molstruc.2019.06.076>
- [65] W.L. Cai, X.L. Weng, Z.L. Chen. Highly efficient removal of antibiotic rifampicin from aqueous solution using green synthesis of recyclable nano-Fe₃O₄. *Environmental Pollution*, 2019, 247: 839–846. <https://doi.org/10.1016/j.envpol.2019.01.108>
- [66] H. Veisi, L. Mohammadi, S. Hemmati, et al. *In situ* immobilized silver nanoparticles on *Rubia tinctorum* extract-coated ultrasmall iron oxide nanoparticles: An efficient nanocatalyst with magnetic recyclability for synthesis of propargylamines by A³ coupling reaction. *ACS Omega*, 2019, 4(9): 13991–14003. <https://doi.org/10.1021/acsomega.9b01720>
- [67] M. Mahmoudi, H. Hofmann, B. Rothen-Rutishauser, et al. Assessing the *in vitro* and *in vivo* toxicity of superparamagnetic iron oxide nanoparticles. *Chemical Reviews*, 2012, 112(4): 2323–2338. <https://doi.org/10.1021/cr2002596>
- [68] N. Asare, C. Instanes, W.J. Sandberg, et al. Cytotoxic and genotoxic effects of silver nanoparticles in testicular

- cells. *Toxicology*, 2012, 291(1-3): 65–72. <https://doi.org/10.1016/j.tox.2011.10.022>
- [69] M.J.H. Dowlath, S.A. Musthafa, S.B. Mohamed Khalith, et al. Comparison of characteristics and biocompatibility of green synthesized iron oxide nanoparticles with chemical synthesized nanoparticles. *Environmental Research*, 2021, 201: 111585. <https://doi.org/10.1016/j.envres.2021.111585>
- [70] M. Nikzamir, A. Akbarzadeh, Y. Panahi. An overview on nanoparticles used in biomedicine and their cytotoxicity. *Journal of Drug Delivery Science and Technology*, 2021, 61: 102316. <https://doi.org/10.1016/j.jddst.2020.102316>
- [71] R. Sheel, P. Kumari, P.K. Panda, et al. Molecular intrinsic proximal interaction infer oxidative stress and apoptosis modulated invivo biocompatibility of P.niruri contrived antibacterial iron oxide nanoparticles with zebrafish. *Environmental Pollution*, 2020, 267: 115482. <https://doi.org/10.1016/j.envpol.2020.115482>
- [72] G.C. Hermosa, C.S. Liao, H.S. Wu, et al. Green synthesis of magnetic ferrites (Fe_3O_4 , CoFe_2O_4 , and NiFe_2O_4) stabilized by aloe vera extract for cancer hyperthermia activities. *IEEE Transactions on Magnetics*, 2022, 58(8): 5400307. <https://doi.org/10.1109/tmag.2022.3158835>
- [73] A.L. Ramirez-Nuñez, L.F. Jimenez-Garcia, G.F. Goya, et al. *In vitro* magnetic hyperthermia using polyphenol-coated $\text{Fe}_3\text{O}_4@ \gamma\text{Fe}_2\text{O}_3$ nanoparticles from *Cinnamomum verum* and *Vanilla planifolia*: The concert of green synthesis and therapeutic possibilities. *Nanotechnology*, 2018, 29(7): 074001. <https://doi.org/10.1088/1361-6528/aaa2c1>
- [74] J. Sandhya, S. Kalaiselvam. Biogenic synthesis of magnetic iron oxide nanoparticles using inedible borassus flabellifer seed coat: Characterization, antimicrobial, antioxidant activity and *in vitro* cytotoxicity analysis. *Materials Research Express*, 2020, 7(1): 015045. <https://doi.org/10.1088/2053-1591/ab6642>
- [75] E.A. Moacă, C.G. Watz, D. Flondor Ionescu, et al. Biosynthesis of iron oxide nanoparticles: Physico-chemical characterization and their *in vitro* cytotoxicity on healthy and tumorigenic cell lines. *Nanomaterials*, 2022, 12(12): 2012. <https://doi.org/10.3390/nano12122012>
- [76] H. Al-Karagoly, A. Rhyaf, H.L. Naji, et al. Green synthesis, characterization, cytotoxicity, and antimicrobial activity of iron oxide nanoparticles using *Nigella sativa* seed extract. *Green Processing and Synthesis*, 2022, 11(1): 254–265. <https://doi.org/10.1515/gps-2022-0026>
- [77] X. Peng, X. Qian, H. Mao, et al. Targeted magnetic iron oxide nanoparticles for tumor imaging and therapy. *International Journal of Nanomedicine*, 2008, 3(3): 311–321. <https://doi.org/10.2147/ijn.s2824>
- [78] X.H. Sun, A. Tan, B.J. Boyd. Magnetically-activated lipid nanocarriers in biomedical applications: A review of current status and perspective. *WIREs Nanomedicine and Nanobiotechnology*, 2023, 15(3): e1863. <https://doi.org/10.1002/wnan.1863>
- [79] M.L. García Martín, P. López Larrubia. Preclinical MRI, vol. 1718. New York, NY: Springer New York, 2018. <https://doi.org/10.1007/978-1-4939-7531-0>
- [80] D.H. Liu, W.T. Yang, B.B. Zhang. Magnetic resonance imaging and its molecular probes in evaluating the response to tumor treatment. *Nano Biomedicine and Engineering*, 2024. <https://doi.org/10.26599/nbe.2024.9290073>
- [81] M. Legacz, K. Roepke, M. Giersig, et al. Contrast agents and cell labeling strategies for *in vivo* imaging. *Advances in Nanoparticles*, 2014, 3(2): 41–53. <https://doi.org/10.4236/anp.2014.32007>
- [82] Y.K. Peng, S.C.E. Tsang, P.T. Chou. Chemical design of nanoprobe for T_1 -weighted magnetic resonance imaging. *Materials Today*, 2016, 19(6): 336–348. <https://doi.org/10.1016/j.mattod.2015.11.006>
- [83] J. Lin, X.H. Ma, A.R. Li, et al. Multiple valence states of Fe boosting SERS activity of Fe_3O_4 nanoparticles and enabling effective SERS-MRI bimodal cancer imaging. *Fundamental Research*, 2024, 4(4): 858–867. <https://doi.org/10.1016/j.fmre.2022.04.018>
- [84] S.J. Chen, L. An, S.P. Yang. Low-molecular-weight Fe(III) complexes for MRI contrast agents. *Molecules*, 2022, 27(14): 4573. <https://doi.org/10.3390/molecules27144573>
- [85] Contents: (Adv. Mater. 11/2017). *Advanced Materials*, 2017, 29(11): 1770074. <https://doi.org/10.1002/adma.201770074>
- [86] D.J. Todd, J. Kay. Gadolinium-induced fibrosis. *Annual Review of Medicine*, 2016, 67: 273–291. <https://doi.org/10.1146/annurev-med-063014-124936>
- [87] H. Malikova, M. Holesta. Gadolinium contrast agents - are they really safe. *The Journal of Vascular Access*, 2017, 18(2_suppl): S1–S7. <https://doi.org/10.5301/jva.5000713>
- [88] M. Rogosnitzky, S. Branch. Gadolinium-based contrast agent toxicity: A review of known and proposed mechanisms. *BioMetals*, 2016, 29(3): 365–376. <https://doi.org/10.1007/s10534-016-9931-7>
- [89] J. Ramalho, R.C. Semelka, M. Ramalho, et al. Gadolinium-based contrast agent accumulation and toxicity: An update. *American Journal of Neuroradiology*, 2016, 37(7): 1192–1198. <https://doi.org/10.3174/ajnr.a4615>
- [90] T. Kanda, K. Ishii, H. Kawaguchi, et al. High signal intensity in the dentate nucleus and globus pallidus on unenhanced T1-weighted MR images: Relationship with increasing cumulative dose of a gadolinium-based contrast material. *Radiology*, 2014, 270(3): 834–841. <https://doi.org/10.1148/radiol.13131669>
- [91] H. Wei, O.T. Bruns, M.G. Kaul, et al. Exceedingly small iron oxide nanoparticles as positive MRI contrast agents. *Proceedings of the National Academy of Sciences of the United States of America*, 2017, 114(9): 2325–2330. <https://doi.org/10.1073/pnas.1620145114>
- [92] S. Taheri, N.J. Shah, G.A. Rosenberg. Analysis of pharmacokinetics of Gd-DTPA for dynamic contrast-enhanced magnetic resonance imaging. *Magnetic Resonance Imaging*, 2016, 34(7): 1034–1040. <https://doi.org/10.1016/j.mri.2016.04.014>
- [93] W.S. Xie, Z.H. Guo, F. Gao, et al. Shape-, size- and structure-controlled synthesis and biocompatibility of iron oxide nanoparticles for magnetic theranostics. *Theranostics*, 2018, 8(12): 3284–3307. <https://doi.org/10.7150/thno.25220>
- [94] D.S. Ling, M.J. Hackett, T. Hyeon. Surface ligands in synthesis, modification, assembly and biomedical applications of nanoparticles. *Nano Today*, 2014, 9(4): 457–477. <https://doi.org/10.1016/j.nantod.2014.06.005>
- [95] N. Lee, D. Yoo, D.S. Ling, et al. Iron oxide based nanoparticles for multimodal imaging and magnetoresponsive therapy. *Chemical Reviews*, 2015, 115(19): 10637–10689. <https://doi.org/10.1021/acs.chemrev.5b00112>
- [96] D.S. Ling, W. Park, S.J. Park, et al. Multifunctional tumor pH-sensitive self-assembled nanoparticles for bimodal imaging and treatment of resistant heterogeneous tumors. *Journal of the American Chemical Society*, 2014, 136(15): 5647–5655. <https://doi.org/10.1021/ja4108287>
- [97] D.S. Ling, N. Lee, T. Hyeon. Chemical synthesis and

- assembly of uniformly sized iron oxide nanoparticles for medical applications. *Accounts of Chemical Research*, 2015, 48(5): 1276–1285. <https://doi.org/10.1021/acs.accounts.5b00038>
- [98] E. Illés, M. Szekeres, I.Y. Tóth, et al. PEGylation of superparamagnetic iron oxide nanoparticles with self-organizing polyacrylate-PEG brushes for contrast enhancement in MRI diagnosis. *Nanomaterials*, 2018, 8(10): 776. <https://doi.org/10.3390/nano8100776>
- [99] A. Lazaro-Carrillo, M. Filice, M.J. Guillén, et al. Tailor-made PEG coated iron oxide nanoparticles as contrast agents for long lasting magnetic resonance molecular imaging of solid cancers. *Materials Science and Engineering: C*, 2020, 107: 110262. <https://doi.org/10.1016/j.msec.2019.110262>
- [100] I. Khmara, O. Strbak, V. Zavisova, et al. Chitosan-stabilized iron oxide nanoparticles for magnetic resonance imaging. *Journal of Magnetism and Magnetic Materials*, 2019, 474: 319–325. <https://doi.org/10.1016/j.jmmm.2018.11.026>
- [101] P. Kharey, M. Goel, Z. Husain, et al. Green synthesis of biocompatible superparamagnetic iron oxide-gold composite nanoparticles for magnetic resonance imaging, hyperthermia and photothermal therapeutic applications. *Materials Chemistry and Physics*, 2023, 293: 126859. <https://doi.org/10.1016/j.matchemphys.2022.126859>
- [102] S. Bano, S. Nazir, A. Nazir, et al. Microwave-assisted green synthesis of superparamagnetic nanoparticles using fruit peel extracts: Surface engineering, T_2 relaxometry, and photodynamic treatment potential. *International Journal of Nanomedicine*, 2016, 11: 3833–3848. <https://doi.org/10.2147/ijn.s106553>
- [103] R.S. Tade, M.P. More. Emerging application of graphene quantum dots in photodynamic/photothermal and hyperthermia therapies for cancer treatment. *Nano Biomedicine and Engineering*, 2024. <https://doi.org/10.26599/nbe.2024.9290083>
- [104] Z. Hedayatnasab, F. Abnisa, W.M.A.W. Daud. Review on magnetic nanoparticles for magnetic nanofluid hyperthermia application. *Materials & Design*, 2017, 123: 174–196. <https://doi.org/10.1016/j.matdes.2017.03.036>
- [105] J. Beik, Z. Abed, F.S. Ghoreishi, et al. Nanotechnology in hyperthermia cancer therapy: From fundamental principles to advanced applications. *Journal of Controlled Release*, 2016, 235: 205–221. <https://doi.org/10.1016/j.jconrel.2016.05.062>
- [106] N. Mahesh, N. Singh, P. Talukdar. Investigation of a breast cancer magnetic hyperthermia through mathematical modeling of intratumoral nanoparticle distribution and temperature elevations. *Thermal Science and Engineering Progress*, 2023, 40: 101756. <https://doi.org/10.1016/j.tsep.2023.101756>
- [107] Szwed, M., Marczak, A. Application of nanoparticles for magnetic hyperthermia for cancer treatment—The current state of knowledge. *Cancers*, 2024, 16(6): 1156. <https://doi.org/10.3390/cancers16061156>
- [108] M. Creixell, A.C. Bohórquez, M. Torres-Lugo, et al. EGFR-targeted magnetic nanoparticle heaters kill cancer cells without a perceptible temperature rise. *ACS Nano*, 2011, 5(9): 7124–7129. <https://doi.org/10.1021/nn201822b>
- [109] E. Obrador, A. Jihad-Jebbar, R. Salvador-Palmer, et al. Externally applied electromagnetic fields and hyperthermia irreversibly damage cancer cells. *Cancers*, 2023, 15(13): 3413. <https://doi.org/10.3390/cancers15133413>
- [110] S. Ebrahimisadr, B. Aslibeiki, R. Asadi. Magnetic hyperthermia properties of iron oxide nanoparticles: The effect of concentration. *Physica C: Superconductivity and Its Applications*, 2018, 549: 119–121. <https://doi.org/10.1016/j.physc.2018.02.014>
- [111] A. Urtizberea, E. Natividad, A. Arizaga, et al. Specific absorption rates and magnetic properties of ferrofluids with interaction effects at low concentrations. *The Journal of Physical Chemistry C*, 2010, 114(11): 4916–4922. <https://doi.org/10.1021/jp912076f>
- [112] I. Hilger. *In vivo* applications of magnetic nanoparticle hyperthermia. *International Journal of Hyperthermia*, 2013, 29(8): 828–834. <https://doi.org/10.3109/02656736.2013.832815>
- [113] R.J. Wydra, P.G. Rychahou, B.M. Evers, et al. The role of ROS generation from magnetic nanoparticles in an alternating magnetic field on cytotoxicity. *Acta Biomaterialia*, 2015, 25: 284–290. <https://doi.org/10.1016/j.actbio.2015.06.037>
- [114] Priya, Naveen, K. Kaur, et al. Green synthesis: An eco-friendly route for the synthesis of iron oxide nanoparticles. *Frontiers in Nanotechnology*, 2021, 3: 655062. <https://doi.org/10.3389/fnano.2021.655062>
- [115] M.F. Horst, D.F. Coral, M.B. Fernández van Raap, et al. Hybrid nanomaterials based on gum Arabic and magnetite for hyperthermia treatments. *Materials Science and Engineering: C*, 2017, 74: 443–450. <https://doi.org/10.1016/j.msec.2016.12.035>
- [116] A. Alkhayal, A. Fathima, A.H. Alhasan, et al. PEG coated Fe₃O₄/RGO nano-cube-like structures for cancer therapy via magnetic hyperthermia. *Nanomaterials*, 2021, 11(9): 2398. <https://doi.org/10.3390/nano11092398>
- [117] N.A. Gharibkandi, M. Žuk, F.Z.B. Muftuler, et al. ¹⁹⁸Au-coated superparamagnetic iron oxide nanoparticles for dual magnetic hyperthermia and radionuclide therapy of hepatocellular carcinoma. *International Journal of Molecular Sciences*, 2023, 24(6): 5282. <https://doi.org/10.3390/ijms24065282>
- [118] M. Vassallo, D. Martella, G. Barrera, et al. Improvement of hyperthermia properties of iron oxide nanoparticles by surface coating. *ACS Omega*, 2023, 8(2): 2143–2154. <https://doi.org/10.1021/acsomega.2c06244>
- [119] A. Rajan, M. Sharma, N.K. Sahu. Assessing magnetic and inductive thermal properties of various surfactants functionalised Fe₃O₄ nanoparticles for hyperthermia. *Scientific Reports*, 2020, 10: 15045. <https://doi.org/10.1038/s41598-020-71703-6>
- [120] V.A.J. Silva, P.L. Andrade, A. Bustamante, et al. Magnetic and Mössbauer studies of fucan-coated magnetite nanoparticles for application on antitumoral activity. *Hyperfine Interactions*, 2014, 224(1): 227–238. <https://doi.org/10.1007/s10751-013-0875-9>
- [121] B. Jang, M.S. Moorthy, P. Manivasagan, et al. Fucoidan-coated CuS nanoparticles for chemo-and photothermal therapy against cancer. *Oncotarget*, 2018, 9(16): 12649–12661. <https://doi.org/10.18632/oncotarget.23898>

© The author(s) 2025. This is an open-access article distributed under the terms of the Creative Commons Attribution 4.0 International License (CC BY) (<http://creativecommons.org/licenses/by/4.0/>), which permits unrestricted use, distribution, and reproduction in any medium, provided the original author and source are credited.